

Outcomes of untreated posterolateral knee injuries: an in vivo canine model

Chad J. Griffith · Coen A. Wijdicks ·
Ute Goerke · Shalom Michaeli · Jutta Ellermann ·
Robert F. LaPrade

Received: 1 September 2010 / Accepted: 6 December 2010 / Published online: 11 January 2011
© Springer-Verlag 2010

Abstract

Purpose The purpose of our study was to determine if sectioning the canine fibular collateral ligament, popliteus tendon, and popliteofibular ligament would result in residual posterolateral instability and produce measurable evidence of early-onset arthritis on ultra-high field MRI.

Methods The fibular collateral ligament, popliteus tendon, and popliteofibular ligament were surgically sectioned in six canines. Six months postoperatively, both limbs were biomechanically tested involving 3.25 Nm varus and 1.25 Nm internal and external rotation torques at 28.5° (mean full extension), 60°, and 90° of flexion. A 7.0-tesla MRI scanner acquired $T_{1\rho}$ -weighted images, and relaxation time constants were calculated.

Results Compared to the non-operative knees, varus angulation significantly increased by 2.0°, 8.0°, and 12.4° in the operative knees at full extension, 60° flexion, and 90° flexion, respectively. External rotation was significantly increased by 8.1° at full extension, 12.2° at 60°, and 8.2° at 90°. Internal rotation was significantly increased by 9.1° at

full extension and 12.4° at 60°. $T_{1\rho}$ MRI mapping revealed a significant increase in relaxation times in the medial compartment of the surgical knees compared to controls.

Conclusion This study validated that grade III surgically created posterolateral knee injuries do not heal and that the canine knee developed early-onset changes of the medial compartment, indicative of early-onset osteoarthritis, developed in the operative knees.

Keywords Posterolateral knee injuries · Canine · Osteoarthritis · Knee instability · 7 Tesla MRI · $T_{1\rho}$ mapping

Introduction

Posterolateral knee injuries [15, 20] are often overlooked because they rarely occur in isolation and, in fact, occur with a concurrent cruciate ligament injury in over 75 percent of cases [19, 29, 30]. The potential to overlook these injuries can lead to further pathology. Untreated grade III posterolateral knee injuries have been demonstrated in humans to not heal and ultimately lead to cruciate ligament graft failure, medial meniscal tears, and medial compartment osteoarthritis due to the increased contact forces in the medial compartment resulting from the increased varus laxity with gait [14, 16–18, 29, 30]. While there is limited long-term information on the natural history of isolated posterolateral knee injuries [16], there have been reports of the deleterious effects of combined posterolateral knee and posterior cruciate ligament injuries on the articular cartilage of the medial compartment of the knee over that found solely with isolated PCL tears [34, 35]. However, it is unknown to what extent chondrocyte degeneration associated with posterolateral knee injuries was due to the initial

Winner of the “Best Poster Award-ESSKA 2010, Oslo Norway”.

C. J. Griffith
Department of Orthopaedic Surgery, University of Minnesota,
Minneapolis, MN, USA

C. A. Wijdicks · R. F. LaPrade (✉)
Biomechanics Research Department, Steadman Philippon
Research Institute, 181 West Meadow Drive, Suite 1000,
Vail, CO 81657, USA
e-mail: drlaprade@sprivaill.org

U. Goerke · S. Michaeli · J. Ellermann
Center for Magnetic Resonance Research,
University of Minnesota, Minneapolis, MN, USA

traumatic event or due to abnormal loads from the knee instability caused by this injury pattern.

Due to the difficulty involved in studying the natural history of untreated posterolateral instability in humans, the availability of a well-characterized animal model is essential. Previous work in this area by our group has focused on attempts to develop such a model in rabbits and goats [21, 22, 31]. Following sectioning of the rabbit posterolateral knee structures, the resultant instability pattern was similar to the human knee [21, 22]. However, the small size of the rabbit knee joints made implementation of repair or reconstruction techniques very difficult [21, 22]. Similarly, while the goat model exhibited a significant increase in posterolateral knee instability *in vitro*, the amount of *in vivo* instability was clinically insignificant, possibly because the fused goat tibiofibula created an inherent bony stability of the lateral knee compartment [31]. A recent *in vitro* study reported that both the anatomy and biomechanics of the canine posterolateral knee were similar to the human knee [11].

Recently, quantitative high-resolution MRI (7 tesla) has been reported to provide a non-invasive and reliable assessment of articular cartilage [6]. Thus, the use of 7-tesla MRI provides a means to longitudinally follow the development of osteoarthritis over time and may help determine if surgical intervention can change the natural history of the development of osteoarthritis.

The hypothesis for this study was that posterolateral knee instability could be created *in vivo* in the canine knee and that medial compartment knee osteoarthritis lesions would develop. Therefore, the purpose of the present study was to determine if sectioning of the fibular collateral ligament, popliteus tendon, and popliteofibular ligament in the canine knee would result in residual posterolateral instability and produce measureable early evidence of medial compartment osteoarthritis of the knee on ultra-high field MRI.

Materials and methods

Six skeletally mature, male, mixed breed canines with a mean age of 358 ± 19 days and mean weight of 26.8 ± 1.3 kg at the time of surgery were utilized for this study. Approval for the study was obtained from the Institutional Animal Care and Use Committee at the University of Minnesota (Approval # 0610A94726). We determined our number of animals to be six, due to a recent *in vitro* study performed in our laboratory found significant differences in both the anatomy and biomechanics of the canine posterolateral knee [11]. A concurrent study assessing this same group of canines to determine the ability of 7.0-Tesla MRI to measure articular cartilage

thickness and area compared to histological sections was also performed and was recently reported [32]. There was one additional canine in this current group compared to the previous study.

Surgical procedure and postoperative care

Alternating right and left limbs were operated on with the contralateral limb used as an unoperated control. After anesthesia induction, a 4-cm longitudinal incision was made lateral and parallel to the patellar tendon to expose the posterolateral structures. The biceps femoris muscle and fascia was exposed and retracted proximally to expose the fibular collateral ligament. Two incisions, anterior and posterior to the fibular collateral ligament, were made and a Kirschner-wire (K-wire) was inserted medial (deep) to the fibular collateral ligament. Several small longitudinal stab incisions were then made in the ligament to weaken it. Brisk lateral traction resulted in a midsubstance mop-end tear of the fibular collateral ligament, and these ends were then left *in situ* similar to a previously reported technique [21, 22, 31]. Similarly, the popliteus tendon and popliteofibular ligament were exposed and ruptured. The small lateral capsular incision was closed, and the skin was closed with a subcuticular stitch.

After 3–5 days of confinement, the dogs were allowed unrestricted activity and exercised twice daily. The canines were housed individually in 1.3 m by 1.8 m cages, fed commercial dog food twice a day, and were provided free choice water.

Biomechanical testing

Humane euthanasia was performed 6 months after the surgical procedure. The knees were prepared for biomechanical testing by severing the leg at the distal tibia, and cementing the proximal femur and distal tibia in polymethylmethacrylate (PMMA). A hexagonal-bolt and lock nut were potted in PMMA along with the distal tibia for application of external forces according to a previously described technique [11]. Biomechanical testing of motion limits for both varus moments and internal-external rotation torques were performed on all operated and control knees using a previously described customized testing apparatus [11], which fixed the femur in a static horizontal static position while allowing uninhibited motion of the tibia/fibula at fixable angles of flexion.

Displacement of the tibia with respect to the static femur was recorded using the Polhemus Liberty system (Polhemus Incorporated, Colchester, VT). This device utilized an alternating current (AC) 6-degree-of-freedom electromagnetic tracking device which captured the coordinate locations and spatial orientations of receivers with respect to a

global positioning transmitter. All experiments were performed at a distance of approximately 200 mm from the transmitter, which was within the optimal accuracy range of 100–700 mm between the sensors and the transmitter [3]. The reported accuracy of this AC tracking device under these test conditions has been reported to be within 0.56° to 0.92° [12]. Two receivers were rigidly attached to the specimen using threaded K-wires at the mid-femur and anterior tibial crest, distal to the tibial tubercle, and a three-dimensional coordinate system for the two receivers was established. The position change of the coordinate systems of the two receivers with respect to each other between pre-testing and posttesting was measured by Motion Monitor computer software (Innovative Sports Training, Chicago, IL).

Each knee was tested in full extension for that individual knee (mean: 28.5° , range $24\text{--}35^\circ$), 60° , and 90° of knee flexion. The following external loads were applied three times at each knee flexion angle and the results averaged: 3.25 Nm of varus torque and 1.25 Nm of internal and external rotation torques. Varus torque was measured by a load cell (Interface Force, Scottsdale, AZ) (manufacturer reported non-repeatability error of $\pm 0.02\%$). Internal and external rotational torques were measured by a 17-kg-cm Torqometer (Snap-on Tools Corporation, Kenosha, WI) with a manufacturer's reported accuracy of $\pm 2\%$.

MRI Measurements

After biomechanical testing was completed, the canine knees were immediately brought to the 7.0-tesla MRI scanner (Siemens, Erlangen, Germany) for analysis. Quadrature surface coils, with separate actively detuned transmits and receives channels, were used for the experiment. This coil provided the best filling factor and the highest signal-to-noise ratio required for $T_{1\rho}$ -mapping. A scout scan was obtained to verify that the coronal plane was perpendicular to the long axis of the tibia. Coronal $T_{1\rho}$ MRI images were then obtained with imaging parameters of a matrix size of $384 \times 288 \times 192$, from which a final matrix size of $384 \times 384 \times 256$ was obtained. Four coronal slices were obtained between the posterior margin of the anterior horn and the anterior margin of the posterior horn of the medial meniscus in all specimens, using partial Fourier reconstruction in the slice and the phase-encoded dimension; echo time, 5.1 ms; repetition time, 16 ms; one average, isotropic resolution 310 micrometer; and acquisition bandwidth, 320 Hz/pixel, with a total imaging time of approximately 15 min.

For the adiabatic $T_{1\rho}$ measurements, images for $T_{1\rho}$ weighting were collected [26, 27] with decay curves measured using adiabatic full passage pulses (AFP) [8] of the hyperbolic secant (HS) family [33] (adiabaticity factor

$R = 20$, pulse time duration was $T_p = 5.12$ ms) placed prior to the Turbo FLASH imaging readout (echo time $TE = 5.1$ ms) [13]. The repetition time between segments was 4 s, number of segments = 4, number of excitation per segment = 33, matrix = 192×196 , $FOV = 12 \times 12$ cm^2 , and the slice thickness was 1.5 mm. The number of pulses in the pulse train = 4, 8, 12, and 16 with the phases prescribed according to MLEV-4 [23] were used. Generation of $T_{1\rho}$ relaxation maps was performed by using pixel-by-pixel analysis with monoexponential decay function using a MATLAB software package (MATLAB 7.0, The MathWorks, Natick, MA). Relaxation time constants were determined from the regions of interest, and average values were calculated. All values are presented in mean \pm standard deviation.

Statistical analysis

Motion differences between varus angulation and internal and external rotation as well as differences of the average $T_{1\rho}$ -values between the operated and control knees were evaluated using a paired Student's two-tailed t test (SAS). Statistical significance was defined as $P < 0.05$.

Results

During the postoperative period, subjective reports from the veterinary technician reported no evidence of limb favoring or limping in any of the canines. All animals had healthy eating habits and either maintained or gained weight over the course of the study.

MRI

$T_{1\rho}$ mapping (Table 1; Fig. 1) revealed a significant increase ($P < 0.01$) in relaxation time in the medial compartments of the surgical knees compared to the controls. The mean increase in relaxation time in the medial compartments of the surgical knees compared to the controls was 33.3%. There was no significant change in $T_{1\rho}$ relaxation times seen in the lateral compartments of any knees.

Table 1 Mean and standard deviation of the $T_{1\rho}$ -MRI relaxation values in the medial and lateral compartment of the control and operated knee joint (units = milliseconds (ms))

$T_{1\rho}$ (ms)	Control (ms)	Surgery (ms)	P value (two-tailed)
Medial	160 ± 30	210 ± 30	0.01
Lateral	190 ± 50	170 ± 60	0.7

The P value represents the statistical significance of the differences between the mean values based on a two-tailed t test

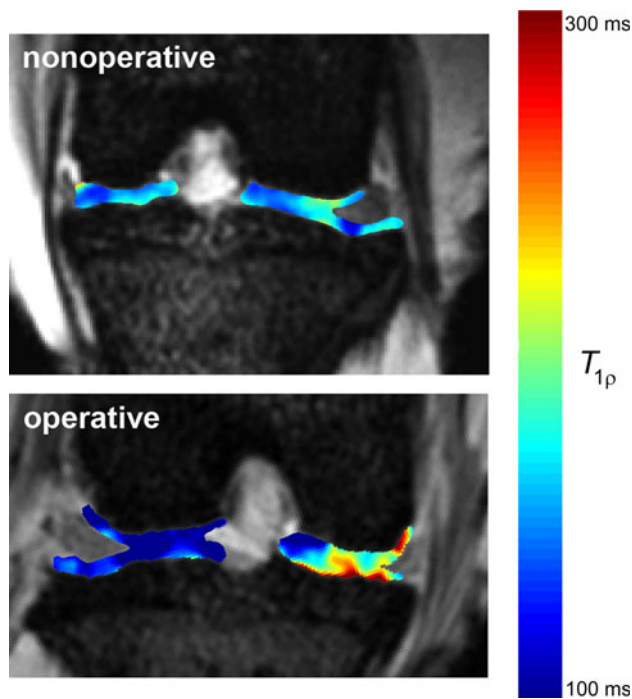


Fig. 1 Images of the color-coded $T_{1\rho}$ -maps superimposed on the articular cartilage of the respective anatomic image. **a** $T_{1\rho}$ MRI on contralateral non-operative knee. **b** $T_{1\rho}$ MRI on left knee with sectioned fibular collateral ligament, popliteofibular ligament, and popliteus tendon. There is an increase of the $T_{1\rho}$ -relaxation times in milliseconds (ms) in the medial compartment of the operative knee versus the non-operative knee

Biomechanical analysis

Compared to the control knees, sectioning of the fibular collateral ligament, popliteus tendon, and popliteofibular ligament significantly increased varus angulation by 2.0° ($P < 0.05$), 8.0° ($P < 0.01$), and 12.4° ($P < 0.001$) at full extension, 60° of knee flexion, and 90° of knee flexion, respectively (Fig. 2). External rotation in the operative knees was significantly increased compared to control knees by 8.1° at full extension ($P < 0.05$), 12.2° at 60° flexion ($P < 0.001$), and 8.2° at 90° flexion ($P < 0.001$) (Fig. 3). Internal rotation significantly increased by 9.1° ($P < 0.05$) in full extension and 12.4° ($P < 0.001$) at 60° , respectively, in the operative compared to the control knees (Fig. 4). Internal rotation at 90° flexion was not significantly different.

Discussion

The most important conclusion of this study was that it was validated that grade III posterolateral knee injuries do not heal and that untreated injuries can lead to early-onset

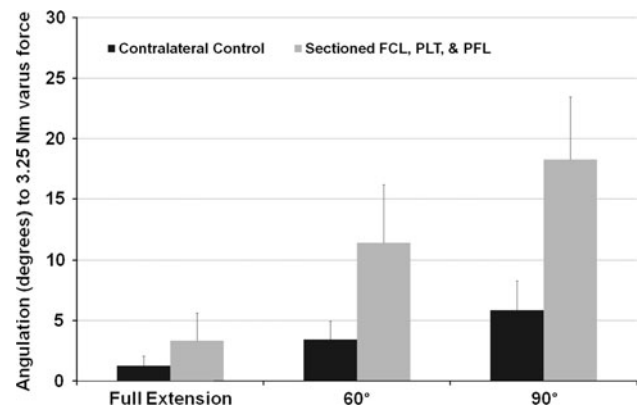


Fig. 2 Graph depicting the increase in varus angulation in knees with a sectioned fibular collateral ligament, popliteus tendon, and popliteofibular ligament compared to the contralateral control knees following the application of a 3.25 Nm varus torque. *FCL* fibular collateral ligament, *PLT* popliteus tendon, *PFL* popliteofibular ligament

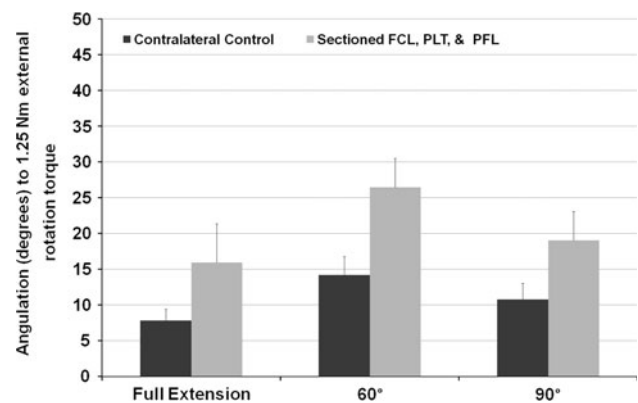


Fig. 3 Graph depicting the increase in external rotation in knees with a sectioned fibular collateral ligament, popliteus tendon, and popliteofibular ligament compared to the contralateral control knees following the application of a 1.25 Nm external rotation torque. *FCL* fibular collateral ligament, *PLT* popliteus tendon, *PFL* popliteofibular ligament

arthritis of the medial compartment of the knee. No healing occurred after sectioning the fibular collateral ligament, popliteus tendon, and popliteofibular ligament in the dog knee after 6 months of unlimited cage activity. In addition, high-field MRI scans demonstrated evidence of early-onset proteoglycan depletion in the medial compartment of the operative knees, indicative of the early phases of osteoarthritis. Thus, it is believed that the canine knee was validated as a model to study the natural history of untreated human posterolateral knee injuries.

The size of the canine knee, the bony instability secondary to the opposing convex surfaces of the lateral femoral condyle and lateral tibial plateau, and the non-fused tibia and fibula, should circumvent the difficulties experienced in the two previous unsuccessful attempts to

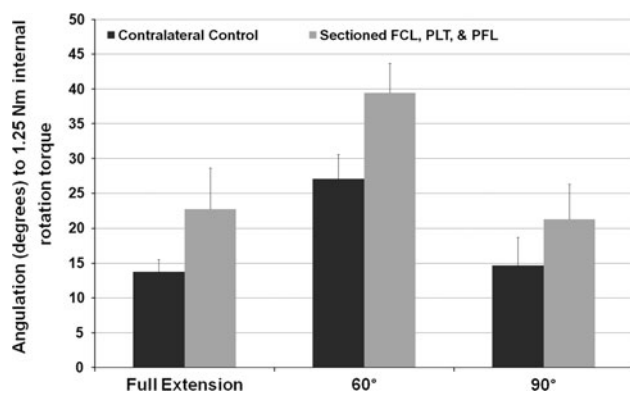


Fig. 4 Graph depicting the increase in internal rotation in knees with a sectioned fibular collateral ligament, popliteus tendon, and popliteofibular ligament compared to the contralateral control knees following the application of a 1.25 Nm internal rotation torque. *FCL* fibular collateral ligament, *PLT* popliteus tendon, *PFL* popliteofibular ligament

develop an appropriate animal model to study the natural history of posterolateral instability of the knee [11, 21, 22, 31]. Similar to a previous *in vitro* canine study [11], sectioning of the fibular collateral ligament, popliteus tendon, and popliteofibular ligament in this *in vivo* study created significant posterolateral instability. This instability resulted in evidence of early-onset osteoarthritis in the medial compartment of the knee, similar to the location where it has been reported in humans [20]. It is theorized that arthritis first develops at this location due to the increased compressive forces which occur medially due to lateral compartment gapping at foot strike. The size and instability of the canine knee should allow for the validation of previous *in vitro* human knee biomechanical studies [14, 18, 20] and for determining the effect that surgical intervention can have on the natural history of untreated posterolateral knee injuries regarding the development and progression of medial compartment osteoarthritis.

This study demonstrated that early-stage articular cartilage degenerative changes in an *in vivo* injury model were able to be demonstrated on a 7.0-tesla MRI scanner. There were significant signal changes seen on $T_{1\rho}$ MRI scans of the medial compartment of the operative knees, which indicated the early depletion of proteoglycan concentration, which correlated with the expected findings for early-onset osteoarthritis as reported by previous studies [1, 4, 5, 7, 24]. Studies have demonstrated that as osteoarthritis begins to develop, the proteoglycan concentration in articular cartilage initially decreases [9, 24], as was found in this study. This proteoglycan concentration decrease is concurrently accompanied by an increase in water content and wet weight [1, 4, 24], which would result in an increase in articular cartilage thickness and area.

It is anticipated that the significant increase in $T_{1\rho}$ relaxation time of the medial compartment found in this

study and the increase in articular cartilage thickness reported in an earlier paper that was detected using both MRI and histology, reflect the development of early osteoarthritic changes in this *in vivo* posterolateral injury canine model. It is well known that during the early development of osteoarthritis, both proteoglycan concentration and binding in articular cartilage initially decreases, and this change has been reported to be accompanied by an increase in water content and wet weight [1, 2, 4, 5, 7, 10, 24, 25, 28]. Previous studies theorized that the increase in water content may be due to a loosening of the collagen matrix of the articular cartilage [10, 24] and is associated with a change in content and organization of type II collagen and proteoglycans [28]. Increases in water content have also been reported to be accompanied by chondrocyte hypertrophy [2, 4], resulting in an increase in articular cartilage thickness by as much as two-fold [4, 25]. Detecting osteoarthritis changes in these early stages is very important because it allows for the potential to measure the effectiveness of potential early treatments to prevent the progressive development of more severe articular cartilage damage.

One of the limitations was there were only six canines in this study. Another limitation was that the knees were only followed to the 6-month postoperative time frame. Further work to utilize increased dog numbers or a longer postoperative time frame to further study the development of osteoarthritis, and if surgical intervention can alter its development, in this animal posterolateral knee injury model would be recommended.

The clinical relevance of this work is that it confirms that grade III posterolateral knee injuries do not heal. This appears due to the unique bony anatomy of the lateral compartment where two opposing convex surfaces articulate with each other. When encountered clinically, grade III posterolateral knee injuries should be treated to avoid the sequelae of ligament instability and the potential development of medial compartment arthritis.

Conclusions

In conclusion, the purpose of developing a large animal *in vivo* posterolateral knee instability model was accomplished, and the hypothesis that untreated posterolateral knee injuries do not heal and lead to the development of early-onset osteoarthritis of the medial compartment of the knee was verified. In addition, this study further validates the clinical observation in humans that unlike medial knee injuries which almost always heal in both animals and humans, grade III posterolateral knee injuries do not heal and that surgical treatment should be considered to prevent the sequelae of chronic posterolateral knee instability.

References

1. Adams ME (1989) Cartilage hypertrophy following canine anterior cruciate ligament transection differs among different areas of the joint. *J Rheumatol* 16:818–824
2. Adams ME, Brandt KD (1991) Hypertrophic repair of canine articular cartilage in osteoarthritis after anterior cruciate ligament transection. *J Rheumatol* 18:428–435
3. An KN, Jacobsen MC, Berglund LJ, Chao EY (1988) Application of a magnetic tracking device to kinesiologic studies. *J Biomech* 21:613–620
4. Appleyard RC, Burkhardt D, Ghosh P, Read R, Cake M, Swain MV, Murrell GA (2003) Topographical analysis of the structural, biochemical and dynamic biomechanical properties of cartilage in an ovine model of osteoarthritis. *Osteoarthritis Cartilage* 11:65–77
5. Calvo E, Palacios I, Delgado E, Ruiz-Cabello J, Hernandez P, Sanchez-Pernaute O, Egido J, Herrero-Beaumont G (2001) High-resolution MRI detects cartilage swelling at the early stages of experimental osteoarthritis. *Osteoarthritis Cartilage* 9:463–472
6. Eckstein F, Burstein D, Link TM (2006) Quantitative MRI of cartilage and bone: degenerative changes in osteoarthritis. *NMR Biomed* 19:822–854
7. Fernandes JC, Martel-Pelletier J, Lascau-Coman V, Moldovan F, Jovanovic D, Raynauld JP, Pelletier JP (1998) Collagenase-1 and collagenase-3 synthesis in normal and early experimental osteoarthritic canine cartilage: an immunohistochemical study. *J Rheumatol* 25:1585–1594
8. Garwood M, DelaBarre L (2001) The return of the frequency sweep: designing adiabatic pulses for contemporary NMR. *J Magn Reson* 153:155–177
9. Goldring D, Levy U, Mendlovic D (2007) Highly dispersive micro-ring resonator based on one dimensional photonic crystal waveguide design and analysis. *Opt Express* 15:3156–3168
10. Goldring MB, Goldring SR (2007) Osteoarthritis. *J Cell Physiol* 213:626–634
11. Griffith CJ, LaPrade RF, Coobs BR, Olson EJ (2007) Anatomy and biomechanics of the posterolateral aspect of the canine knee. *J Orthop Res* 25:1231–1242
12. Griffith CJ, LaPrade RF, Johansen S, Armitage B, Wijdicks C, Engebretsen L (2009) Medial knee injury: part I, static function of the individual components of the main medial knee structures. *Am J Sports Med* 37:1762–1770
13. Haase A (1990) Snapshot flash MRI: application to t1-, t2-, and chemical shift imaging. *Magn Reson Med* 13:77–89
14. Harner CD, Vogrin TM, Hoher J, Ma CB, Woo SL (2000) Biomechanical analysis of a posterior cruciate ligament reconstruction. Deficiency of the posterolateral structures as a cause of graft failure. *Am J Sports Med* 28:32–39
15. Hughston JC, Andrews JR, Cross MJ, Moschi A (1976) Classification of knee ligament instabilities. Part II. The lateral compartment. *J Bone Joint Surg Am* 58:173–179
16. Kannus P (1989) Nonoperative treatment of grade II and III sprains of the lateral ligament compartment of the knee. *Am J Sports Med* 17:83–88
17. LaPrade RF, Muench C, Wentorf F, Lewis JL (2002) The effect of injury to the posterolateral structures of the knee on force in a posterior cruciate ligament graft: a biomechanical study. *Am J Sports Med* 30:233–238
18. LaPrade RF, Resig S, Wentorf F, Lewis JL (1999) The effects of grade III posterolateral knee complex injuries on anterior cruciate ligament graft force. A biomechanical analysis. *Am J Sports Med* 27:469–475
19. LaPrade RF, Terry GC (1997) Injuries to the posterolateral aspect of the knee. Association of anatomic injury patterns with clinical instability. *Am J Sports Med* 25:433–438
20. LaPrade RF, Wentorf F (2002) Diagnosis and treatment of posterolateral knee injuries. *Clin Orthop Relat Res* 33:110–121
21. LaPrade RF, Wentorf FA, Crum JA (2004) Assessment of healing of grade III posterolateral corner injuries: an in vivo model. *J Orthop Res* 22:970–975
22. LaPrade RF, Wentorf FA, Olson EJ, Carlson CS (2006) An in vivo injury model of posterolateral knee instability. *Am J Sports Med* 34:1313–1321
23. Levitt M, Freeman R, Frenkel T (1982) Broadband heteronuclear decoupling. *J Magn Reson* 47:328–330
24. Little CB, Ghosh P, Bellenger CR (1996) Topographic variation in biglycan and decorin synthesis by articular cartilage in the early stages of osteoarthritis: an experimental study in sheep. *J Orthop Res* 14:433–444
25. McDevitt C, Gilbertson E, Muir H (1977) An experimental model of osteoarthritis; early morphological and biochemical changes. *J Bone Joint Surg Br* 59:24–35
26. Michaeli S, Sorce DJ, Garwood M (2008) T-2 rho and t-1 rho adiabatic relaxations and contrasts. *Current Analytical Chemistry* 4:8–25
27. Michaeli S, Sorce DJ, Springer CS Jr, Ugurbil K, Garwood M (2006) T1rho mri contrast in the human brain: modulation of the longitudinal rotating frame relaxation shutter-speed during an adiabatic rf pulse. *J Magn Reson* 181:135–147
28. Miosge N, Hartmann M, Maelicke C, Herken R (2004) Expression of collagen type I and type II in consecutive stages of human osteoarthritis. *Histochem Cell Biol* 122:229–236
29. Noyes FR, Barber-Westin SD, Albright JC (2006) An analysis of the causes of failure in 57 consecutive posterolateral operative procedures. *Am J Sports Med* 34:1419–1430
30. O'Brien SJ, Warren RF, Pavlov H, Panariello R, Wickiewicz TL (1991) Reconstruction of the chronically insufficient anterior cruciate ligament with the central third of the patellar ligament. *J Bone Joint Surg Am* 73:278–286
31. Olson EJ, Wentorf FA, McNulty MA, Parker JB, Carlson CS, LaPrade RF (2008) Assessment of a goat model of posterolateral knee instability. *J Orthop Res* 26:651–659
32. Pepin SR, Griffith CJ, Wijdicks CA, Goerke U, McNulty MA, Parker JB, Carlson CS, Ellermann J, LaPrade RF (2009) A comparative analysis of 7.0-tesla magnetic resonance imaging and histology measurements of knee articular cartilage in a canine posterolateral knee injury model: a preliminary analysis. *Am J Sports Med* 37(1):119S–124S
33. Silver M, Joseph R, Hoult D (1984) Highly selective $\pi/2$ and π pulse generation. *J Magn Reson* 59:347–351
34. Skyhar MJ, Warren RF, Ortiz GJ, Schwartz E, Otis JC (1993) The effects of sectioning of the posterior cruciate ligament and the posterolateral complex on the articular contact pressures within the knee. *J Bone Joint Surg Am* 75:694–699
35. Strobel MJ, Weiler A, Schulz MS, Russe K, Eichhorn HJ (2003) Arthroscopic evaluation of articular cartilage lesions in posterior-cruciate-ligament-deficient knees. *Arthroscopy* 19:262–268